CRYSTAL GROWTH & DESIGN

Article

Cite This: Cryst. Growth Des. 2019, 19, 3348−3357

pubs.acs.org/crystal

Cu(II) and Zn(II) Complexes with Dinitrobenzoates and Pyrazolyl Ligands: Structural and Thermal Stability Influence of N−H Moiety

Juan F. Torres,[†] Mario A. Macías,[†] Sebastian Franco-Ulloa,[‡] Gian Pietro Miscione,[‡] Justo Cobo,[§] and John J. Hurtado*[,†]

[†]Department of Chemistry, Universidad de los Andes, Carrera 1 No. 18A-12, 111711 Bogotá, Colombia

[‡]COBO Computational Bio-Organic Chemistry Bogotá, Chemistry Department, Universidad de los Andes, Cra 1 No 18A-12, 111711 Bogotá, Colombia

[§]Department of Inorganic and Organic Chemistry, Universidad de Jaén, 23071 Jaén, Spain

Supporting Information

ABSTRACT: The synthesis and characterization of air-stable Cu(II) and Zn(II) complexes with 3,5-dinitrobenzoate (DNB) and 3,5-dimethylpyrazole (L1) or bis(3,5-dimethylpyrazol-1-yl)methane (L2) are described. Three of these complexes exhibit a monomeric structure, while the Cu(II) complex with L2 is a trinuclear complex. Density functional theory calculations were performed to understand the unexpected formation of the three-centered compound. In agreement with the X-ray crystal structure, the N−H moiety present in L1 was identified as possible driving force to obtain monomeric structures, while L2, without it, can favor the trinuclear complex formation. Thermal studies were carried for the complexes, and it was observed that the presence of the azole ligand allows the decomposition of the complexes at lower temperatures due to the presence of acidic protons, being especially important for L1.

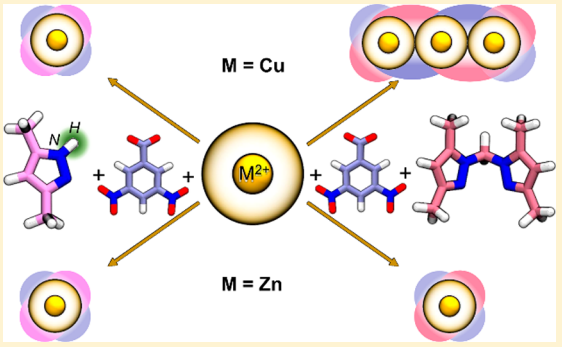

1. INTRODUCTION

3,5-Dinitrobenzoate (DNB) is a versatile ligand that presents a wide variety of coordination modes in which the carboxylate and nitro groups can be involved.[1] Complexes with DNB and different metal centers have been extensively studied, demonstrating the flexibility of DNB as an anionic ligand. Among these compounds, Cu(II) and Zn(II) complexes have been synthesized and found to exhibit rich structural diversity. Indeed, monomers,[2−11] dimers,[1,11,12] and polymers[1,13−15] of copper and zinc with DNB and different coligands can be found in the literature. However, few reports have been published showing Cu(II) and Zn(II) complexes containing DNB and azole ligands. A zinc complex with 3,5-dimethylpyrazole and DNB was previously studied.[16] This complex and its copper analogue were proven useful as initiators for the ring opening polymerization (ROP) of ε-caprolactone and D,L-lactide, obtaining polycaprolactone (PCL) and polylactide (PLA) respectively.[17] In the same way, another zinc complex was synthesized using DNB and 3,5-diphenylpyrazole ligands, and it was used as a catalyst for the ring opening copolymerization of cyclohexene oxide with carbon dioxide.[18]

Recently, an interest in controlled PCL synthesis[19] has increased due to PCL biodegradability, miscibility with other polymers, and mechanical properties.[20] PCL has been used in tissue engineering, drug delivery systems, and microelectronics, among others.[20] Specifically, PCL can be used for the production of biodegradable packaging, which is of environmental interest.[21] Therefore, we started studies of Cu(II) and Zn(II) complexes with DNB and pyrazolyl ligands searching for active catalysts for ROP of ε-caprolactone.[22]

During the synthesis of complexes containing 3,5-dimethylpyrazole (L_1) and bis(3,5-dimethyl-1-pyrazolyl)methane (L_2), we found an unexpected copper trinuclear formation (Scheme 1), which motivated a detailed study of these compounds. Herein, we report the synthesis and spectroscopic and thermal studies of Cu(II) and Zn(II) complexes containing DNB and azole ligands, as well as the molecular structure determined by single-crystal X-ray diffraction for three of them. Additionally, we present a computational study in order to understand the copper trinuclear formation. Our results suggest that hydrogen bonding involving the N−H moiety in L_1 is a relevant driving force to obtain monomeric structures, while its absence in L_2 results in greater stabilization of trinuclear species. We also found that the acidic protons in the pyrazolyl ligands affect strongly the thermal stability of the complexes.

Received: February 23, 2019
Revised: April 3, 2019
Published: April 19, 2019

DOI: 10.1021/acs.cgd.9b00246
Cryst. Growth Des. 2019, 19, 3348−3357

Scheme 1. Synthesis of Copper and Zinc Complexes with 3,5-Dinitrobenzoates and Pyrazolyl Ligands

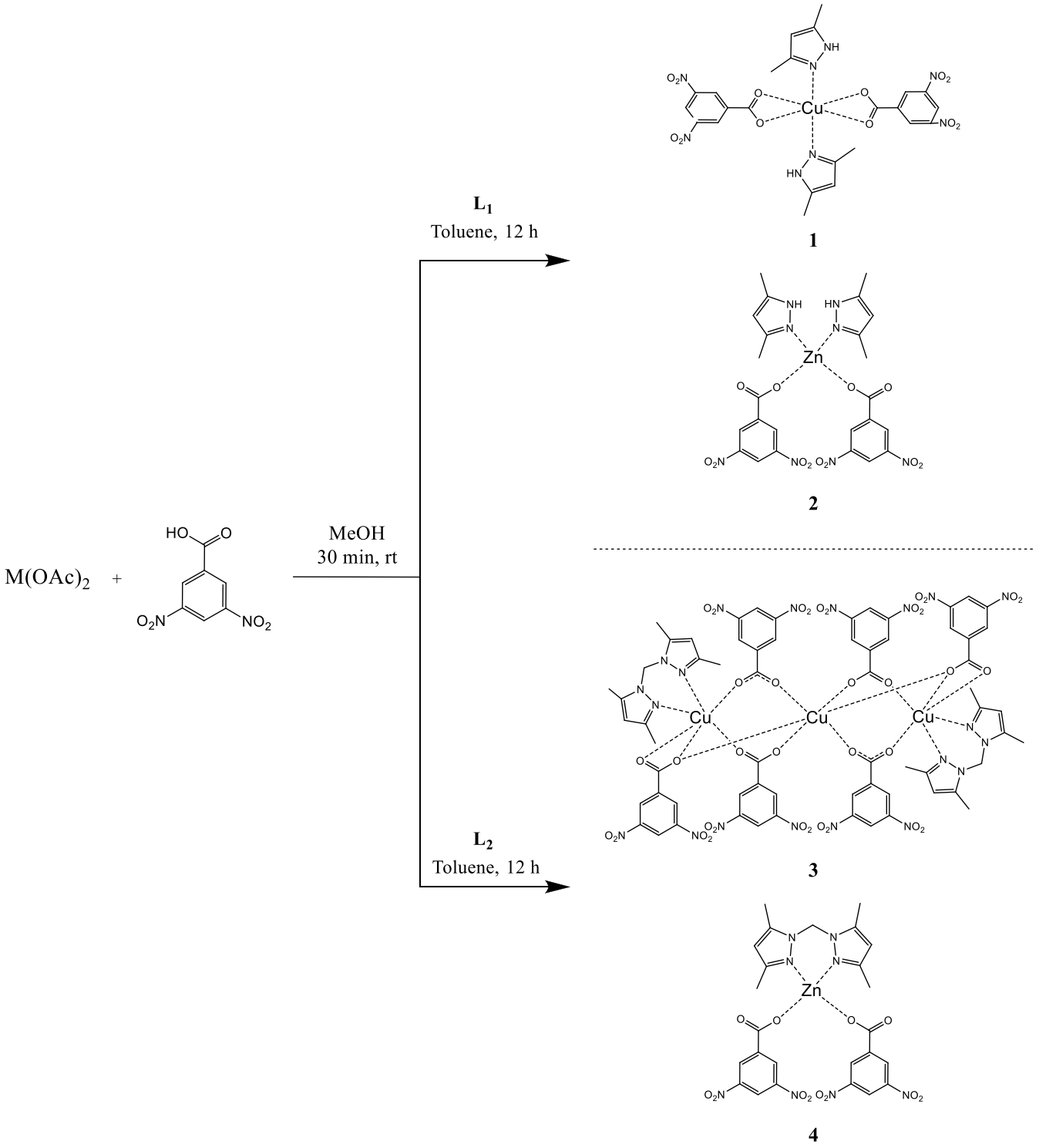

2. EXPERIMENTAL SECTION

2.1. Materials and Instruments. All the reagents and solvents were obtained from commercial sources and were used without further purification. 3,5-Dimethylpyrazole (L_1) was acquired from Sigma-Aldrich, and bis(3,5-dimethyl-1-pyrazolyl)methane (L_2) was synthesized as described in the literature.[23] Elemental analysis (C, H, and N) were determined with a Thermo Scientific FLASH 2000 CHNS/O Analyzer. Fourier transform infrared (FTIR) spectra were recorded on a Thermo Nicolet NEXUS FTIR spectrophotometer using KBr pellets from 500 to 4000 cm^{-1}. Ultraviolet/visible (UV/vis) spectra were recorded in an Agilent Technologies Cary 100 spectrophotometer by dissolving the copper complexes in THF. The wavelength was scanned from 300 to 900 nm. Melting points were determined on a Mel-Temp 1101D apparatus in open capillary tubes and was reported without corrections. Nuclear magnetic resonance (NMR) spectra were recorded in dimethyl sulfoxide-*d* (DMSO-*d*) on a BrukerAscend-400 spectrometer, and chemical shifts are reported in δ(ppm) relative to TMS. Thermogravimetric (TG) analysis of the complexes were obtained on a NETZSCH STA 409 PC/PG in nitrogen media. The samples were subjected to dynamic heating over a temperature range of 30−695 °C with a heating rate of

DOI: 10.1021/acs.cgd.9b00246
Cryst. Growth Des. 2019, 19, 3348−3357

10 °C min^{-1}. The TG curves were analyzed to give the percentage of lost mass as a function of the temperature.

2.2. Synthesis and Characterization of Complexes. The complexes were prepared by modified literature procedures.[17] In a round-bottom flask metal(II) acetate was dissolved in 15 mL of methanol. Two equivalents of 3,5-dinitrobenzoic acid were added and stirred for 30 min at room temperature. Then, a toluene solution (10 mL) of the azole ligand was added into the flask and stirred for 12 h at room temperature. The formed solid was collected, washed with methanol, and dried under vacuum.

2.2.1. Complex ***1****, [Cu(DNB)$_2$(L$_1$)$_2$].* After the reaction finished and no solid was observed, it was necessary to remove solvent until near dryness conditions before continuing with the purification process. A purple solid was obtained from the reaction between Cu(OAc)$_2$ (0.20 g, 1.00 mmol), 3,5-dinitrobenzoic acid (0.43 g, 2.00 mmol), and L$_1$ (0.19 g, 2.00 mmol). Yield: 0.486 g (72%). Mp 216−217 °C. FTIR (KBr) (ν, cm^{-1}): 3194(m), 3141(m), 3114(s), 3049(m), 2880(w), 1614(s), 1580(s), 1541(s), 1462(s), 1424(m), 1395(s), 1344(s), 1301(m), 1191(w), 1071(m), 920(m), 788(s), 722(s), 436(w). UV/vis λ_{max}(nm) (ε, cm^2 mol^{-1}): 712 (1.11 × 10^5). Anal. Calcd. for $C_{24}H_{22}CuN_8O_{12}$: (%) C 42.51, H 3.27, N 16.53. Found: C 41.94, H 3.23, N 15.91.

2.2.2. Complex ***2****, [Zn(DNB)$_2$(L$_1$)$_2$].* A white solid was obtained from the reaction between Zn(OAc)$_2$ (0.18 g, 1.00 mmol), 3,5-dinitrobenzoic acid (0.43 g, 2.00 mmol), and L$_1$ (0.19 g, 2.00 mmol). Yield: 0.435 g (64%). Mp 208−210 °C. FTIR (KBr) (ν, cm^{-1}): 3101(w), 2872(w), 1626(s), 1570(s), 1543(s), 1460(m), 1386(s), 1344(s), 1297(w), 1191(w), 1053(m), 922(w), 813(w), 723(s), 429(w).NMR (400 MHz, DMSO) ^{1}H 8.95 (d, J = 2.1 Hz, 4H), 8.94−8.93 (m, 2H), 5.82 (s, 2H), 2.16 (s, 12H). Anal. Calcd. for $C_{24}H_{22}ZnN_8O_{12}$: (%) C 42.40, H 3.26, N 16.48. Found: C 42.62, H 3.27, N 16.09.

2.2.3. Complex ***3****, [Cu$_3$(DNB)$_6$(L$_2$)$_2$].* A pale blue solid was obtained from the reaction between Cu(OAc)$_2$ (0.20 g, 1.00 mmol), 3,5-dinitrobenzoic acid (0.43 g, 2.00 mmol), and L$_2$ (0.205 g, 2.00 mmol). Yield: 0.392 g (63%). Mp 266−267 °C (decomposition). FTIR (KBr) (ν, cm^{-1}): 3448(w, broad), 3098(m), 1637(s), 1622(s), 1587(m), 1541(s), 1461(s), 1394(s), 1345(s), 1284(m), 1186(w), 1075(m), 921(w), 789(m), 728(s), 680(w). UV/vis λ_{max}(nm) (ε, cm^2 mol^{-1}): 713 (5.05 × 10^5). Anal. Calc. for $C_{64}H_{50}Cu_3N_{20}O$:[36] (%) C 41.20, H 2.7, N 15.01. Found: C 40.71, H 2.68, N 14.12.

2.2.4. Complex ***4****, [Zn(DNB)$_2$L$_2$].* A white solid was obtained from the reaction between Zn(OAc)$_2$ (0.18 g, 1.00 mmol), 3,5-dinitrobenzoic acid (0.43 g, 2.00 mmol), and L$_2$ (0.205 g, 2.00 mmol). Yield: 0.452 g (65%). Mp 245−246 °C. FTIR (KBr) (ν, cm^{-1}): 3445(w, broad), 3098(w), 1640(s), 1542(s), 1462(m), 1394(m), 1345(s), 1284(w), 1074(w), 921(w), 792(w), 727(s). NMR (400 MHz, DMSO) ^{1}H 8.95−8.92 (m, 6H), 6.03 (s, 2H), 5.81 (s, 2H), 2.39 (s, 6H), 2.05 (s, 6H). Anal. Calcd. for $C_{25}H_{22}ZnN_8O_{12}$: (%) C 43.40, H 3.20, N 16.19. Found: C 43.35, H 3.18, N 15.89.

2.3. X-ray Crystallography. Crystals of suitable size and quality for single crystal X-ray diffraction analysis were obtained by slow evaporation of THF (for **1**) or DCM (for **2** and **4**) solutions of the respective compounds, and by vapor diffusion of diethyl ether into a THF solution of compound **3**. Data collection and refinement details are given in Table S1. All the non-hydrogen atoms were refined anisotropically, while the hydrogen atoms were generated geometrically, placed in calculated positions (C−H = 0.93−0.98 Å; N−H = 0.86 Å) and included as riding contributions with isotropic displacement parameters set at 1.2−1.5 times the U_{eq} value of the parent atom. The crystal structures were refined using the program SHELXL2014;[24] in the case of **1**, it was analyzed as three twin domains from the analysis with Twinrotmat in PLATON. Data for complexes **1**, **3**, and **4** were deposited at CCDC with reference 1882206, 1886341, and 1886342 respectively.

Powder samples were analyzed using X-ray powder diffraction at room temperature using a Miniflex-Rigaku X-ray diffractometer working in Bragg−Brentano geometry with Cu−K$_{\alpha1,2}$ (1.5406 and 1.54439 Å) wavelengths. The diffractometer was operated over an angular range of 2θ = 2°−60° with a step size of 0.02° (2θ). The data analysis was performed by the Le Bail method using the Jana-2006 program (http://jana.fzu.cz/).[25] The process of refinement was carried out assuming a pseudo-Voigt function for peak shape and a calculated background using a linear interpolation between a set of fixed points. The whole patterns were completely explained using the single crystal information suggesting that the crystallographic data are representative of the bulk samples (Supporting Information).

2.4. Theoretical Calculations. Density functional theory (DFT) computations were performed with the Gaussian09 series of programs.[26] The M06 functional proposed by Truhlar and Zhao[27−30] was used in all computations. This functional can provide a reliable description of transition metals and medium-range $\pi-\pi$ interactions at the same time.[31−33] The 6-31+G* basis set, included in the Gaussian package, was used for all atoms except the copper and zinc atoms, which was described with the energy-adjusted pseudopotential basis set proposed by Preuss and co-workers (denoted as sdd pseudopotentials in the Gaussian09 formalism).[34]

3. RESULTS AND DISCUSSION

3.1. Synthesis and Computational Studies. The synthesis of the four complexes were done using a one-pot reaction in which the formation of the 3,5-dinitrobenzoate of the metal was allowed before the addition of the pyrazolyl ligands. Three monomers and one trinuclear species were obtained as shown in Scheme 1. Except for complex **1**, the products precipitate directly from the reaction mixture in moderate yields.

Computational studies were performed to obtain some insights about the unexpected formation of the trinuclear copper species **3** in comparison with the monomeric behavior observed for the other complexes. DFT calculations were used to evaluate the energy of four model systems per each metal: (1A) three interacting mononuclear complexes M(DNB)$_2$(L$_1$)$_2$; (1B) one trinuclear complex [M$_3$(DNB)$_6$(L$_1$)$_4$] and two noninteracting L$_1$; (2A) three interacting mononuclear complexes M(DNB)$_2$L$_2$; (2B) one trinuclear complex [M$_3$(DNB)$_6$(L$_2$)$_2$] and one noninteracting L$_2$. With this, we aimed at understanding if the system is thermodynamically favored to form the trinuclear complex or the corresponding mononuclear one. Since the number of atoms of the trinuclear species is not the same as that of three mononuclear adducts, to be able to compare the energy of the two systems, two L$_1$ and one L$_2$ were included in model systems 1B and 2B, respectively. These free ligands would be interacting with the trinuclear adduct in the true system; however, since the exact mode of this interaction is unknown, calculations were performed on the isolated ligands and their energy summed to the trinuclear complexes energy.

The results of the calculations are summarized in Table 1. It is clear that the trinuclear situation is strongly disfavored when the ligand is the 3,5-dimethylpyrazole (L$_1$). This is particularly true when the metal is zinc, being the trinuclear complex (plus two non interacting L$_1$) 56.82 kcal mol^{-1} higher in energy than the corresponding three mononuclear adduct. The energy difference reduces to more than a half with copper but also in

Table 1. Relative Energy of the Model Systems (Values Are Reported in kcal mol^{-1})

model system	Zn	Cu
1A	0.00	0.00
1B	+56.82	+25.28
2A	0.00	0.00
2B	+4.71	+0.50

DOI: 10.1021/acs.cgd.9b00246
Cryst. Growth Des. 2019, 19, 3348−3357

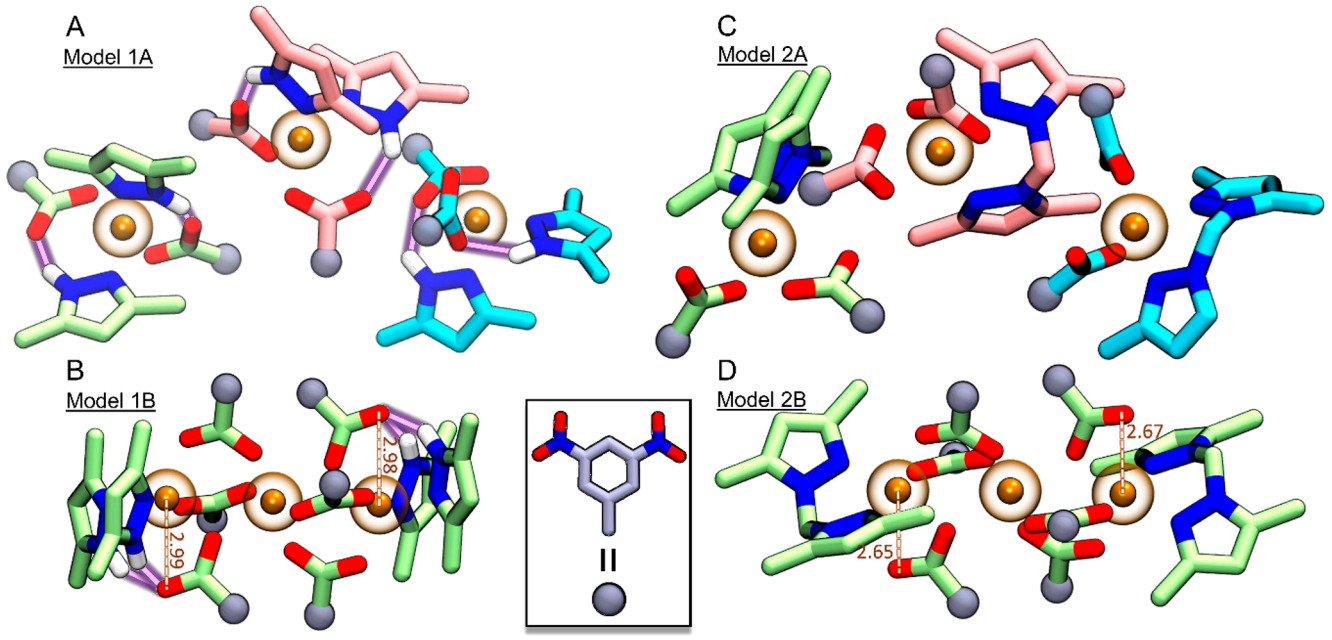

Figure 1. Optimized structures for the model systems when the ligands are coordinated to copper: (A) Model system 1A, (B) model system 1B, (C) model system 2A, and (D) model system 2B. Carbon atoms are displayed in different colors (green, pink, and cyan) for different molecular entities, and copper atoms are drawn in amber. Hydrogen bond networks are shown in purple and copper−oxygen distances are displayed in orange. Hydrogen atoms are omitted for clarity. The hydrogen bond networks disappear, and the copper−oxygen bonds are shortened in the presence of L2 as compared to L1.

this case the thermodynamic is unfavorable for the trinuclear complex formation. This outcome can be rationalized based on both hydrogen-bonding interactions and the metal coordination environment (Figure 1A). The presence of the N−H moiety in L_1 allows strong hydrogen bonds with the carboxylate oxygen atoms in the monomer situation as it can be seen in the crystal structures (vide infra). These noncovalent interactions are mainly intramolecular for zinc and intermolecular for copper. In both cases, the trinuclear complexes present a reduction in the number and strength of the H-bonds with respect to the mononuclear one (Figure 1B). Furthermore, in the trinuclear complex, while the central metal features a hexa-coordinated geometry, the lateral metals are interacting with five ligands only. In fact, one oxygen atom of the DNB carboxylate shows a favorable hydrogen bond with the N−H group of the 3,5-dimethylpyrazole. This reduces the M−O interaction as it can be seen from their bond lengths, which are around 3 Å in the optimized trinuclear model system with L_1 (Figure 1B).

The scenario dramatically changes with the ligand bis(3,5-dimethyl-1-pyrazolyl)methane (L_2). In this case, the energy of trinuclear complexes is just a few kcal mol^{-1} higher than the mononuclear situation. In particular, the formation of the copper trinuclear and mononuclear species have an energy difference of only 0.50 kcal mol^{-1}. The dramatic change in comparison with the L_1 system can be attributed to the fact that there is no N−H acidic proton in L_2, thus the trinuclear formation does not require the cleavage of strong hydrogen bonding interactions (Figure 1C). Additionally, despite the interaction between one DNB's carboxylate oxygen atom and each lateral metal is not so strong (M−O distances are around 2.6 Å, Figure 1D), each metal is coordinated by six ligands. This structural observation particularly favors copper, which accepts more readily electron density than zinc.

Importantly, as clarified above, the interaction between the trinuclear complex and the additional ligands is not explicitly considered in the calculations. It is plausible that such contacts occur through weak electrostatic interactions that may be worth a couple of kcal mol^{-1}. Therefore, the trinuclear and the mononuclear species formation with L_2 can result almost thermodynamically equivalent, or the formation of the trimer can even be favored. It is noteworthy that, for copper, both possible species are sufficiently close in energy and that the observed trimer can be the result of a Le Chatelier displacement of the equilibrium due to the low solubility of complex **3**.

3.2. Spectroscopic Characterization. Table 2 and Figures S1−S4 show FTIR spectroscopic characterization.

Table 2. Spectroscopic Characterization of Complexes

complex	FTIR ν (cm^{-1})			
1	3114(s)	1614(s)	1344(s)	436(w)
2	3101(w)	1626(s)	1344(s)	429(w)
3	3098(m)	1637(s); 1622(s)	1345(s)	-
4	3098(w)	1640(s)	1345(s)	-

The spectra of the complexes exhibited bands that could be related with both DNB and azole ligands. In the range 3098−3114 cm^{-1}, each complex showed a band corresponding to the C−H bond stretching of methyl groups in the pyrazolyl ligands.[35] In the region between 2800 and 3300 cm^{-1}, complexes **1** and **2** show more bands than **3** and **4**, and with higher relative intensities. This could be explained by the presence of the N−H group in L_1, which allows strong hydrogen bond interactions.[35] The carbonyl bands shifted significantly to lower wave numbers for all complexes compared with free 3,5-dinitrobenzoic acid (DNBH), which appears at 1703 cm^{-1}.[36] These shifts in the C═O band

DOI: 10.1021/acs.cgd.9b00246
Cryst. Growth Des. 2019, 19, 3348−3357

Table 3. Thermal Analysis Results of Complexes[a]

					mass loss (%)		
compound	TG range (°C)	DTG_{max} (°C)	*n*	assignment	estimated	calculated	residue
1	168−359	209.9, 335.1	2	loss of 2 DNBH	64.57	62.57	$C_5H_6CuN_2$
	360−695	-	-	loss of L_1	10.83	14.18	
2	167−451	233.9, 417.7	2	loss of 2 DNBH	61.41	61.31	$C_{10}H_6ZnN_4$
	452−695	-	-	partial loss of L_1	-	-	
3	204−311	269.6	1	loss of 5 DNBH	55.10	56.84	$C_{22}H_{26}Cu_3N_8$
	312−695	329.8, 481.6	2	loss of DNBH	13.48	11.37	
4	215−444	242.5, 418.9	2	loss of 2 DNHB	61.41	61.31	$C_{11}H_{14}ZnN_4$
	445−695	-	-	partial loss of L_2	-	-	

[a]TG: thermogravimetric analysis. DTG: derivative thermogravimetric. *n*: number of decomposition steps. DNBH: 3,5-dinitrobenzoic acid. L_1: 3,5-dimethylpyrazole. L_2: bis(3,5-dimethyl-1-pyrazolyl)methane.

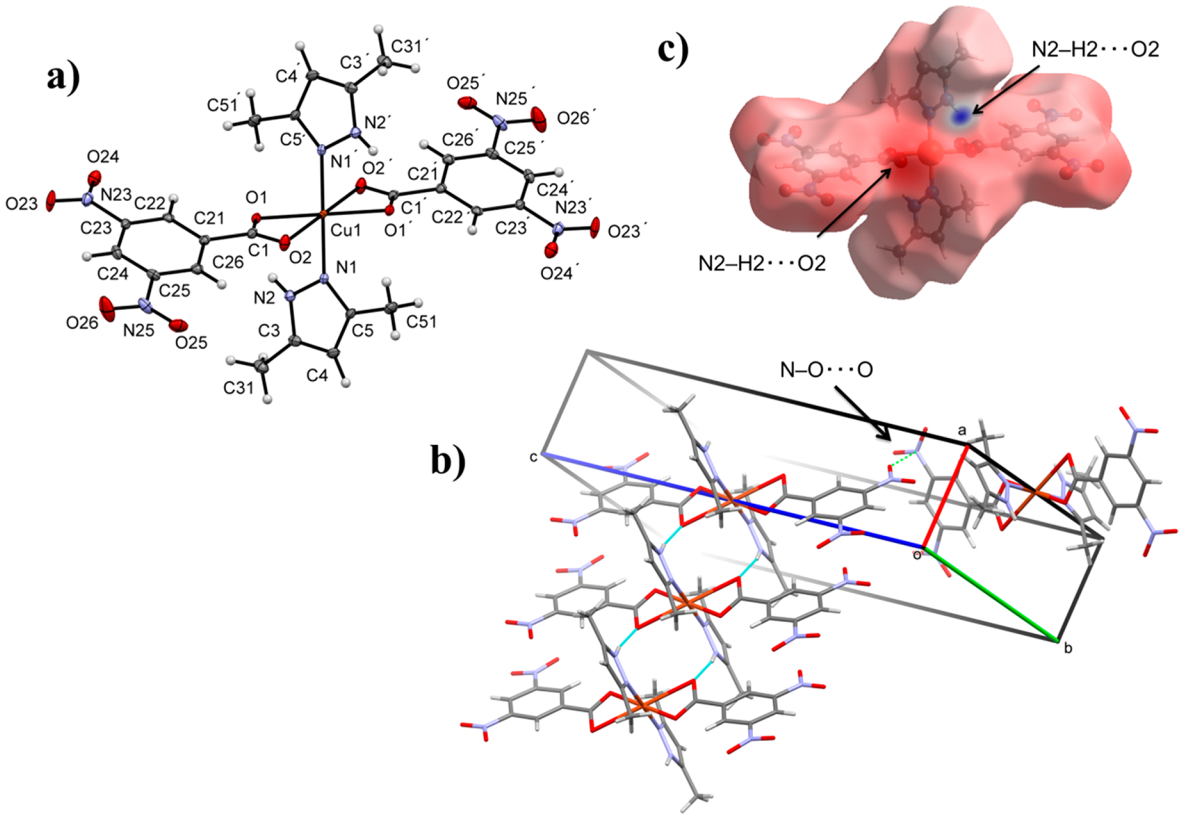

Figure 2. (a) ORTEP plot of $[Cu(DNB)_2(L1)_2]$ showing displacement ellipsoids drawn at the 50% probability level. H atoms are shown as small gray spheres of arbitrary radii. (b) Crystal structure showing the intermolecular N−H···O hydrogen-bonding interactions along the [100] direction and the perpendicular NO···ON interaction (N25−O25···N23). (c) View of the Hirshfeld surface mapped over the electrostatic potential with positive and negative potential indicated in blue and red, respectively. Selected bond lengths (Å): Cu1−O1 1.9894(18), Cu1−O2 2.605(2), Cu1−N1 1.963(2). Selected bond angles (deg): O1−Cu1−O2 55.80(6), O1−Cu1−N1 89.70(8), O1−Cu1−O2 124.20(6), O1−Cu1−N1′ 90.30(8).

absorption are evidence of the coordination and indicate less rigidity in the carbonyl bond in the complexes. For zinc complexes, it was observed that the C═O band in **4** shows slightly a larger wavenumber than **2**. This may indicate that the L_2 ligand supplements metal charge deficiency better than L_1. This trend was also found for copper complexes **1** and **3**. However, the comparison cannot be done directly because they have very different coordination spheres. The trinuclear **3** has two carbonyl bands that are consistent with the structure. In the four complexes the N−O stretching bands of the nitro groups at 1344−1345 cm^{-1} were observed. In all cases the bonds' vibration were found at almost the same frequency, and the observed shifts are less than 5 cm^{-1} compared with free 3,5-dinitrobenzoic acid,[36] suggesting that the NO_2 group is not directly involved in the coordination. Finally, the compounds **1** and **2** present a band in the region 429−436 cm^{-1} corresponding to the out of plane N−H bond bending.[35]

The UV/vis spectra for both copper complexes (Figures S5 and S6) shows an absorption band in the same region of visible light for **1** and **3**, but with a molar attenuation coefficient 4.5 times greater for the trinuclear. This can be expected from a d^9 metal in a six-coordinated environment with only one d−d transition allowed. The fact that complex **3** has a larger molar attenuation coefficient correlates with the presence of more metal centers in the complex.

The NMR spectra of **2** (Figure S7) shows only one signal for the methyl hydrogens of pyrazole, indicating that coordination does not inhibit the tautomerism observed in N−H

DOI: 10.1021/acs.cgd.9b00246
Cryst. Growth Des. 2019, 19, 3348−3357

pyrazoles.[37] This indicates that the interaction between L_1 and zinc is weaker than the interaction between L_2 and zinc, reinforcing the observations from the FTIR analysis. In **4**, the NMR spectra (Figure S8) shows the same signals as those observed for the free azole ligand.[23] All the other hydrogen signals were assigned in accordance with what was expected for the complexes.

3.3. Thermal Analysis. The stages of decomposition, temperature ranges, and weight loss percentages and their assignments are given in Table 3. All the assignments are proposals based on weight loss percentages because detection was not possible. For the four complexes, a residue was obtained after heating above 695 °C, which was not observed in copper and zinc dinitrobenzoates.[1] Furthermore, without the azole ligands the complexes showed high thermal stability until explosion temperature, which ranged from 330 to 410 °C.[1] Compounds **1**−**4** show the loss of 3,5-dinitrobenzoic acid allowed by the presence of acidic hydrogens in pyrazolyl ligands. Complexes containing L_1 may start their decomposition at a lower temperature because the hydrogen in the N−H bond is more acidic than the hydrogens in L_2. After the loss of DNBH, complexes **1**, **2**, and **4** present a constant decreasing in mass that could be assigned to a partial loss of the azole ligand, while complex **3** may not show loss of the pyrazolyl ligand. In addition, complex **3** shows a mass loss between 86 and 203 °C corresponding to the loss of lattice solvent, which was not taken into account for the analysis.

3.4. X-ray Structural Characterization. The crystallographic analysis of the four complexes was performed using the structural information obtained from single crystal X-ray diffraction experiments. A summary of the crystal data is shown in Table S1. In the case of the complex **2**, it was found that this compound crystallizes in triclinic white crystals, space group *P*, with cell parameters values of a = 11.4270(10) Å, b = 11.6473(15) Å, c = 12.4742(10) Å, α = 77.776(5)°, β = 78.362(3)°, and γ = 62.006(4)°, which is in agreement with the crystallographic information previously reported for the same structure.[16]

3.4.1. Structure of Complex ***1*** *[$Cu(DNB)_2(L_1)_2$].* The complexation of the ligands L1 and 3,5-dinitrobenzoate toward the central copper atom gave a mononuclear six-coordinated cationic complex with a coordination sphere containing two pyrazoles (bonded through the N5 atom) and DNB ligands (bonded through the carboxylate group) oriented in a *trans* configuration and with a polyhedral volume of 12.845 Å.[3] The coordination of the DNB ligands is best described as bidentate, while a monodentate behavior is observed for the pyrazole moieties (Figure 2a); the asymmetric unit is half of the complex with the copper atom in half occupancy laying in the inverse center of symmetry at (0,0,1/2) with only one moiety of DNB and pyrazole in the asymmetric unit. The respective pairs of ligands are then reproduced by the inversion through the copper atom. Therefore, they fall in the same plane for each one, forming the pyrazole and dinitrobenzoate rings into a dihedral angle between their least-squares planes of 71.35(14)°, leaving them nearly orthogonal to each other. The bidentate interaction of the DNB with the Cu(II) atom involves both oxygen atoms from the carboxylate groups, however with different bond forces since the Cu−O distances have values of 1.9894(18)Å for Cu1−O1 and 2.605(2) Å for Cu1−O2.[17,38−40] This bis-bidentate carboxylate coordination is rather rarely observed when searching for similar complexes reported in the Cambridge Structural database (CSD Version 5.37 with two updates).[41] However, such coordination is possible due to the *trans* configuration of the ligands in order to preclude steric hindrance.[22] Despite the bidentate nature of the DNB ligands, there are differences in the strength of the Cu−O interactions as a consequence of the C═O character in both carbon−oxygen bonds of the carboxylate groups, considering that the longest Cu−O bond corresponds to the shortest C−O bond (C1−O1 = 1.262(3) Å and C1−O2 = 1.242(3) Å). The difference in the Cu−O bonds is also related to the dihedral angle O2−C1−C21−C22 with a value of 160.0(2)° as a result of the noncoplanar orientation of the carboxylate group with the main plane of the DNB ligand.

Analyzing the supramolecular assembly (Figure 2b), it is possible to observe pairs of inversion related-molecules connected by two equivalent intermolecular N2−H2···O2^{i} hydrogen bonds [symmetry code: (i) −1 + x, y, z] with N−H, H···O, N···O, and N−H···O values of 0.86 Å, 1.88 Å, 2.714(3), and 165.0°, respectively, forming the slabs of infinite chains of molecules running along [100] direction. Each molecule in a slab connects to two translation-equivalent molecules (through a 2-fold screw axis with [010] direction) using weaker C4−H4···O23^{ii} [symmetry code: (ii) x, 1/2 − y,1/2 + z] interactions, with H···O length of 2.817 Å, to join neighboring chains in the [001] and [010] directions. These sort of interactions were observed for an analogue trans complex that contains 4-methoxybenzoate instead of 3,5-dinitrobenzoate,[39] suggesting a great importance of this noncovalent interaction in the stabilization of the structure.

The strong nature of the N2−H2···O2 hydrogen bond allows to imagine an intermolecular attraction collaborating with the weakness of the Cu1−O2 bond allowing even to consider a possible square planar geometry in the coordination sphere leaving the O2 atom participating mainly in the definition of the three-dimensional molecular array. The packing (Figure 2b) shows a peculiar perpendicular NO_2−NO_2 interaction involving the N2−O5···N6 atoms with O···N distance of 2.862(3) Å and N25−O25−N23 angle of 148.4(2)°. Such interesting solid state architecture is helped by these nonbonding interactions between the nitro-groups (being both donor and acceptor groups) of neighboring molecules involving π-hole interactions.[42] These intermolecular N···O interactions involving nitro groups in crystal engineering were previously shown by Gagnon et al. in the X-ray structures of hexakis(4-nitrophenyl)benzene.[43]

In order to observe these intermolecular interactions, electrostatic potentials were calculated using TONTO[44,45] and were mapped on Hirshfeld (HF) surfaces[46] using the STO-3G basis set at the Hartree−Fock level of theory over a range of ±0.30 au. In Figure 2c, the donors are represented with positive potential (blue regions) and the acceptors with negative potential (red regions). The positive potential appears as an intense-blue spot over the N2−H2 atoms, which is consistent with the intense-red cloud over the O2 atom confirming the intermolecular hydrogen bond and its strength, becoming this noncovalent interaction in the most important force participating in the supramolecular assembly.

3.4.2. Structure of Complex ***3*** *[$Cu_3(DNB)_6(L_2)_2$].* The crystallographic data of the complex is summarized in Table S1. In the crystal, the copper cations present two independent coordination geometries with the Cu(1) in a six-coordinated geometry bonded to six oxygen atoms, each one from the carboxylate groups of six different dinitrobenzoates, which are acting as bidentate ligands with each oxygen atom bonded to

DOI: 10.1021/acs.cgd.9b00246
Cryst. Growth Des. 2019, 19, 3348−3357

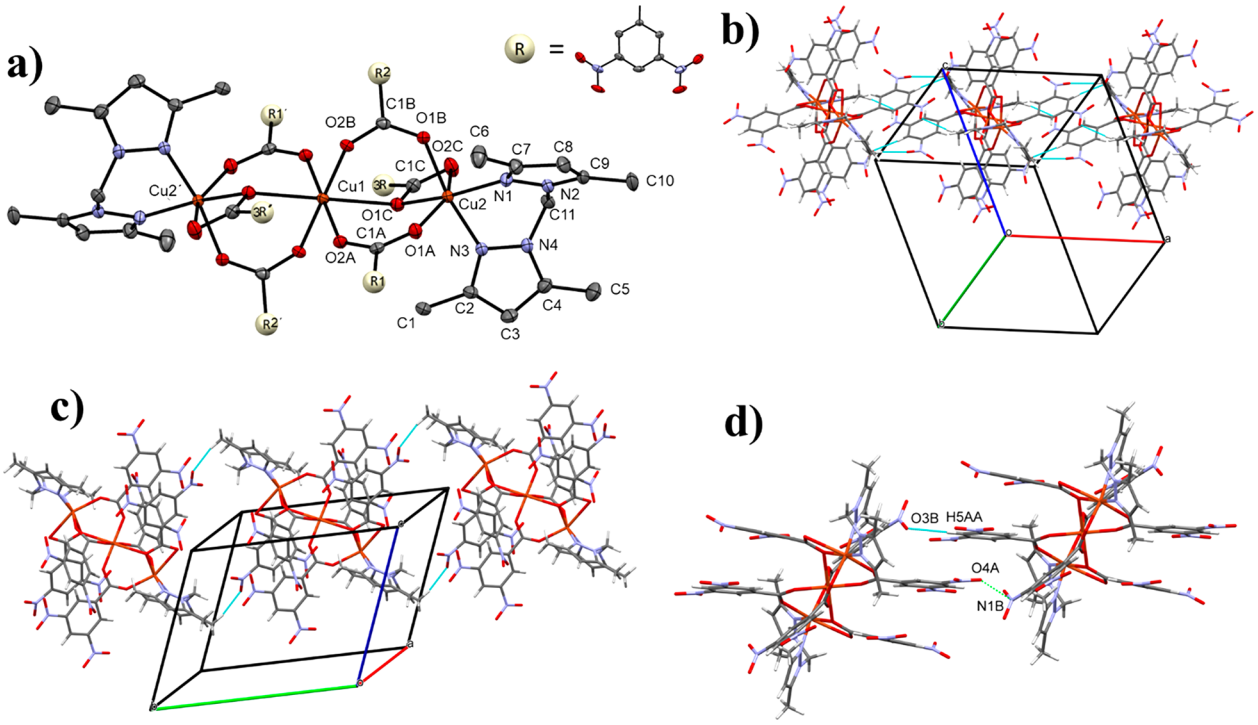

Figure 3. (a) ORTEP plot of $[Cu_3(DNB)_6(L_2)_2]$ showing displacement ellipsoids drawn at the 50% probability level (only the asymmetric unit is numbered). H atoms are omitted, and the dinitrobenzoate rings are represented as R for clarity. (b,c) Crystal structure showing the intermolecular C−H···O hydrogen-bonding interactions along the (b) [100] and (c) [010] directions. (d) Perpendicular NO···ON interaction (N1A−O4A···N1B). Selected bond lengths (Å): Cu1−O1C 2.4784(19), Cu1−O2A 1.9494(17), Cu1−O2B 1.968(2), Cu2−O1A 2.182(2), Cu2−O1B 1.955(2), Cu2−O1C 2.0051(17), Cu2−O2C 2.601(2), Cu2−N1 2.026(2), Cu2−N3 2.002(2). Selected bond angles (deg): O1C−Cu1−O2A 93.83(7), O1C−Cu1−O2B 88.60(7), O2A−Cu1−O2B 96.04(8), O1A−Cu2−O1B 94.20(8), O1A−Cu2−O1C 97.89(8), O1A−Cu2−N1 96.52(8), O1A−Cu2−N3 97.84(9), O1B−Cu2−O1C 90.52(8), O1B−Cu2−O2C 87.08(8), O1B−Cu2−N1 87.75(9).

different metallic centers (Figure 3a). The octahedral polyhedron has an average volume of 12.577 Å^3 and a mean octahedral quadratic elongation of λ = 1.032. The Cu(2) center has also a six-coordination geometry formed by the bonding with three DNB ligands, one acting as bidentate and two as monodentate, and one bis(3,5-dimethylpyrazol-1-yl) methane ligand (L) with both pyrazolyl units bonded to Cu(2) acting as a bidentate ligand. The formed polyhedron has an average volume of 11.801 Å^3 and a mean octahedral quadratic elongation of λ = 1.070, leaving this octahedron with Cu(2) center in a more distorted coordination.[47] This linear trinuclear complex is constituted by two Cu(2) atoms and one Cu(1) atom joined by DNB ligands that act as bridges among these metallic centers, a characteristic rarely observed on similar complexes.[48−51] Considering the chelate rings formed by the connection of L_2 ligands with the Cu(2) centers, the Cu2−N1−N2−C11−N4−N3 rings (the one represented in the asymmetric unit and the one generated by the application of the inversion center at the Cu(1) atom) adopt a boat conformation with puckering parameters Q = 0.809(2) Å, θ = 87.59(14)°, and φ = 1.28(18)° with the Cu(2) and C(11) atoms deviated to the same side of the main plane by 0.4803(10) Å/0.453(3) Å, values that are not too far from those observed in other complexes formed with the bis(3,5-dimethylpyrazol-1-yl) methane ligand allowing to conclude that the structural conformation of this chelating ring results similarly in different systems despite the differences in the coordination number and the length of the coordinated bonds.[52,53] The molecular conformation is also supported by the formation of the intramolecular C(1, 6, 7C, 11)−H(1B, 6C, 7C, 11A)···O(1C, 1A, 1B, 2B, 2C) hydrogen interactions with H···O values within the interval 2.38−2.59 Å, which makes of this contact strong enough to help in the formation of the observed molecular structure.

In order to conform the octahedral coordination in the metallic centers, the orientation of the DNB ligands is such that the least-squares planes that contain the benzene rings are forming dihedral angles of 42.30(15)° for R1−R2 and 49.13(14)° for R2−R3. In the crystal structure, the molecular assembly is controlled mainly by strong C−H···O hydrogen bonds. In the [100] direction (Figure 3b), the trinuclear molecules are connected by a combination of C5B−H5BA···O6C^{i} [H···O = 2.35 Å; symmetry code: (i) 1 + x, y, z] and C1−H1C···O6B^{ii} [H···O = 2.39 Å; symmetry code: (ii) −1 + x, y, z] hydrogen bonds to form infinite chains along the a-axis of the unit cell and involving, in this case, only the DNB ligands. Parallel chains are further connected along [001] by C5A−H5AA···O3B^{iii} [H···O = 2.48 Å; symmetry code: (iii) −1 + x, y, −1 + z] hydrogen bonds to form [010] sheets. The three-dimensional array is completed by the nearly orthogonal C10−H10B···O4C^{iv} [H···O = 2.55 Å; symmetry code: (iv) 1 − x, −y, 2 − z] hydrogen interactions to joint neighboring sheets along b-axis of the unit cell. Along [100] and [001] directions, the DNB ligands are responsible for the supramolecular assembly, while along [010] direction (Figure 3c), intermolecular interactions involving DNB and L_2 ligands help to maintain the three-dimensional organization. This observation allows to establish the great importance of the DNB moieties in the architecture of the crystal, which is also corroborated by the occurrence of a peculiar perpendicular NO_2−NO_2

DOI: 10.1021/acs.cgd.9b00246
Cryst. Growth Des. 2019, 19, 3348−3357

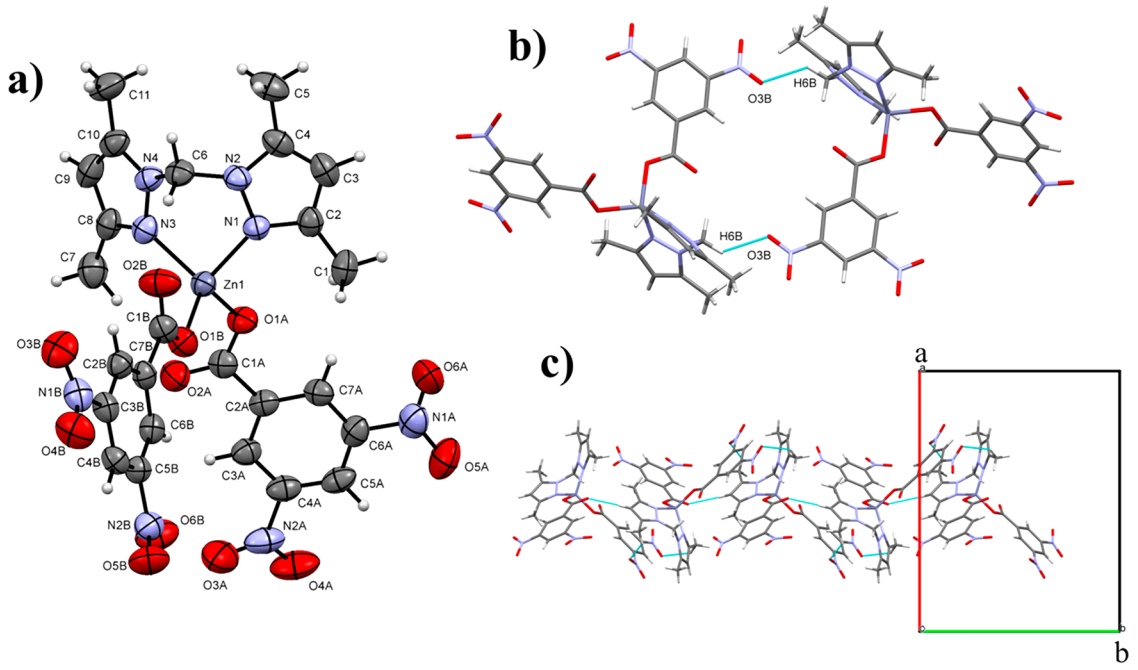

Figure 4. (a) ORTEP plot of $[Zn(DNB)_2(L1)_2]$ showing displacement ellipsoids drawn at the 50% probability level. (b) Pair of inversion-related molecules connected by two equivalent C6−H6B···O3 hydrogen bonds. (c) Crystal structure showing the intermolecular C−H···O hydrogen-bonding interactions along the [001] direction. Selected bond lengths (Å): Zn1−O1A 1.939(2), Zn1−O1B 1.936(3), Zn1−N1 2.036(3), Zn1−N3 2.039(3). Selected bond angles (deg): O1A−Zn1−O1B 103.95(11), O1A−Zn1−N1 103.70(11), O1A−Zn1−N3 119.63(11), O1B−Zn1−N1 118.83(11), O1B−Zn1−N3 116.54(12), N1−Zn1−N3 94.16(11).

interaction (Figure 3d), as mentioned above for $[Cu(DNB)_2(L_1)_2]$ complex, involving the N1A−O4A···N1B atoms and forming a nonbonding connection with O···N distance of 2.814(4) Å and N1A−O4A−N1B angle of 144.1(3)°.

3.4.3. Structure of Complex 4 $[Zn(DNB)_2(L_1)_2]$. The complexation of the ligands bis(3,5-dimethylpyrazol-1-yl)-methane and 3,5-dinitrobenzoate toward the Zn(II) ion gave a mononuclear four-coordinate cationic complex with the coordination sphere formed by two N atoms from both pyrazolyl units and two DNB groups acting as monodentate ligands (Figure 4a). The metallic center forms a tetrahedron with an average volume of 3.863 $Å^3$ and a mean tetrahedral quadratic elongation of λ = 1.029. As seen, the chelate ring adopts a boat conformation with puckering parameters Q = 0.682(3) Å, θ = 82.5(3)°, and φ = 183.4(3)°, values that are in agreement with those previously observed.[52,53] In this conformation, the Zn(1) and C(6) atoms are deviated to the same side of the main plane by −0.3533(12) Å/−0.426(4) Å, respectively. The DNB ligands are present in a conformation described by the dihedral angle formed between the least-squares planes that contain the C(2A, 2B)−C(3A, 3B)−C(4A, 4B)−C(5A, 5B)−C(6A, 6B)−6(7A, 7B) rings with a value of 66.70(17)°. The molecular conformation is also influenced by the intramolecular C1−H1A···O1A, C6−H6A···O2B, and C7−H7C···O2A interactions with H···O lengths of 2.58, 2.22, and 2.38 Å, respectively. In the crystal structure, a combination of C3−H3···O2A^{i} and C7−H7A···O4B^{i} [symmetry code: (i) 1 − x, −1/2 + y, 3/2 − z, H···O lengths of 2.43 and 2.56 Å, respectively] hydrogen bonds join molecules to form infinite chains that run along [010] direction (Figure 4c). Inversion-related chains are further connected by C6−H6B···O3B^{ii} [symmetry code: (ii) 1 − x, 1 − y, 2 − z, H···O length of 2.45 Å] hydrogen interactions to build the molecular assembly along the [001] direction (Figure 4b). In order to construct the three-dimensional array, a combination of C1−H1B···O5B^{iii} [symmetry code: (iii) 1/2 − x, −1/2 + y, z, H···O length of 2.58 Å] and C4B−H4B···O4A^{iv} [symmetry code: (iv) 1/2 − x, 1 − y, 1/2 + z, H···O length of 2.60 Å] hydrogen interactions are involved to connect parallel chains along [100] direction, which are related by a glide plane perpendicular to the a-axis of the unit cell. The supramolecular assembly in the $[Zn(DNB)_2(L_1)_2]$ complex is controlled by classic intermolecular interactions showing no evidence about the existence of NO_2−NO_2 contacts as observed above.

4. CONCLUSIONS

We have synthesized and characterized air-stable copper(II) and zinc(II) complexes with 3,5-dinitrobenzoate and an azole ligand: 3,5-dimethylpyrazole (L_1) or bis(3,5-dimethylpyrazol-1-yl)methane (L_2). Three monomers and an unexpected trinuclear copper complex were obtained. The computational studies and X-ray crystal structures supported the importance of the N−H moiety as relevant driving force to obtain monomeric structures, while the bidentate ligand L_2, without the N−H group, can favor the trinuclear complexes formation. Also, the presence of the azole ligand has a huge impact in the thermal properties by allowing the complexes to lose DNBH and preventing the explosion observed for Cu(II) and Zn(II) dinitrobenzoates.[1] This can be rationalized by the presence of acidic protons in the azole ligand, being the N−H moiety present in L_1 is responsible for a lower decomposition temperature.

■ ASSOCIATED CONTENT

Supporting Information

The Supporting Information is available free of charge on the ACS Publications website at DOI: 10.1021/acs.cgd.9b00246.

DOI: 10.1021/acs.cgd.9b00246
Cryst. Growth Des. 2019, 19, 3348−3357

Recorded spectra, TGA, LeBail analysis, crystallographic data summary, and computed Cartesian coordinates of the computational models (PDF)

Accession Codes

CCDC 1882206 and 1886341−1886342 contain the supplementary crystallographic data for this paper. These data can be obtained free of charge via www.ccdc.cam.ac.uk/data_request/cif, or by emailing data_request@ccdc.cam.ac.uk, or by contacting The Cambridge Crystallographic Data Centre, 12 Union Road, Cambridge CB2 1EZ, UK; fax: +44 1223 336033.

AUTHOR INFORMATION

Corresponding Author

*E-mail: jj.hurtado@uniandes.edu.co.

ORCID

John J. Hurtado: 0000-0002-0511-9719

Notes

The authors declare no competing financial interest.

ACKNOWLEDGMENTS

The authors thank the Universidad de los Andes, Science Faculty and Chemistry Department for providing funding (Convocatoria Facultad de Ciencias 2019−2020), as well as the "Fondo de Apoyo para Profesores Asistentes" of the Universidad de los Andes, Bogotá (Colombia) for financial support. We acknowledge the High-Performance Computing Center of the Universidad de los Andes, Bogotá (Colombia). J.C. thanks Centro de Instrumentación Científico-Técnica of the Universidad de Jaén (UJA) and its staff for the data collection. J.C. thanks the Consejería de Economía, Innovación, Ciencia y Empleo (Junta de Andalucía, Spain) and UJA for financial support.

REFERENCES

(1) Jassal, A. K.; Sharma, S.; Hundal, G.; Hundal, M. S. Structural Diversity, Thermal Studies, and Luminescent Properties of Metal Complexes of Dinitrobenzoates: A Single Crystal to Single Crystal Transformation from Dimeric to Polymeric Complex of Copper(II). *Cryst. Growth Des.* **2015**, *15* (1), 79−93.

(2) Miminoshvili, É. B.; Miminoshvili, K. É.; Adeishvili, G. P. Synthesis and Structure of Trans-Diaquabis(Dimethylsulfoxide)Bis-(3,5-Dinitrobenzoato)Copper(II). *J. Struct. Chem.* **2006**, *47* (1), 91−96.

(3) Fonari, A.; Leonova, E. S.; Antipin, M. Y. On Justification of Cu(II) Environment in Mononuclear Complexes: Joint X-Ray and AIM Studies. *Polyhedron* **2011**, *30* (10), 1710−1717.

(4) Sundberg, M. R.; Klinga, M.; Uggla, R. Unexpected Five-Coordination in Di(1,3-Diaminopropane)-3,5-Dinitrobenzoatocopper(II) 3,5-Dinitrobenzoate. Comparison between the Coordinated and Non-Coordinated Anions. *Inorg. Chim. Acta* **1994**, *216* (1−2), 57−63.

(5) Maroszová, J.; Stachová, P.; Vasková, Z.; Valigura, D.; Koman, M. (3,5-Dinitro-benzoato-KO)Bis-[(2-Pyrid-yl)Methanol-K_2N,O]-Copper(II) 3,5-Dinitro-benzoate. *Acta Crystallogr., Sect. E: Struct. Rep. Online* **2006**, *62* (1), m109−m110.

(6) Zhang, C.-X.; Zhang, Y.-Y.; Sun, Y.-Q. Synthesis, Structures and Magnetic Properties of Copper (II) and Cobalt (II) Complexes Containing Pyridyl-Substituted Nitronyl Nitroxide and 3,5-Dinitrobenzoate. *Polyhedron* **2010**, *29* (5), 1387−1392.

(7) Vasková, Z.; Kitanovski, N.; Jagličić, Z.; Strauch, P.; Růžičková, Z.; Valigura, D.; Koman, M.; Kozlevčar, B.; Moncol, J. Synthesis and Magneto-Structural Characterization of Copper(II) Nitrobenzoate Complexes Containing Nicotinamide or Methylnicotinamide Ligands. *Polyhedron* **2014**, *81*, 555−563.

(8) Kumar, R.; Obrai, S.; Jassal, A. K.; Hundal, M. S.; Mitra, J.; Sharma, S. Synthesis, Structure, Computational, Antimicrobial and in Vitro Anticancer Studies of Copper(II) Complexes with N,N,N′,N′-Tetrakis(2-Hydroxyethyl)Ethylenediamine and Tris(2-Hydroxyethyl)Amine. *J. Coord. Chem.* **2015**, *68* (12), 2130−2146.

(9) Miminoshvili, E. B.; Sobolev, A. N.; Sakvarelidze, T. N.; Miminoshvili, K. E.; Kutelia, E. R. Di-aqua-bis-(Di-methyl Sulfoxide)-bis(3,5-Di-nitro-benzoato)-zinc(II) and the Synthesis of the Cu, Ni and Co Analogs. *Acta Crystallogr., Sect. C: Cryst. Struct. Commun.* **2003**, *59* (4), m118−m120.

(10) Roy, S.; Bauza, A.; Frontera, A.; Schaper, F.; Banik, R.; Purkayastha, A.; Reddy, B. M.; Sridhar, B.; Drew, M. G. B.; Das, S. K.; et al. Structural Diversity and Non-Covalent Interactions in Cd(II) and Zn(II) Complexes Derived from 3,5-Dinitrobenzoic Acid and Pyridine: Experimental and Theoretical Aspects. *Inorg. Chim. Acta* **2016**, *440*, 38−47.

(11) Dey, D.; Roy, S.; Dutta Purkayastha, R. N.; Pallepogu, R.; McArdle, P. Zinc Carboxylates Containing Diimine: Synthesis, Characterization, Crystal Structure, and Luminescence. *J. Mol. Struct.* **2013**, *1053*, 127−133.

(12) Stachová, P.; Moncol, J.; Valigura, D.; Lis, T. Unusual O-Coordination of Caffeine in Tetra-kis(μ-3,5-Dinitro-benzoato-K2$_O$:O′)Bis-[(Caffeine-KO)Copper(II)]. *Acta Crystallogr., Sect. C: Cryst. Struct. Commun.* **2006**, *62* (8), m375−m377.

(13) Hökelek, T.; Mert, Y.; Ünalerouğlu, C. Catena-Poly[[Tetrakis-(μ-3,5-Dinitrobenzoato-O:O′)Dicopper(II)]Bis[(μ-3,5-Dinitrobenzoato-O:O′)(Methanol-O)Copper(II)]]. *Acta Crystallogr., Sect. C: Cryst. Struct. Commun.* **1998**, *54* (3), 310−313.

(14) Yang, G.; Zhu, H.-G.; Zhang, L.-Z.; Cai, Z.-G.; Chen, X.-M. Synthesis, Structure and Second Harmonic Effect of Bis(Mu2−3,5-Dinitrobenzoato-O,O′)Zinc(II) and Tetraaquabis(3,5-Dinitrobenzoato-O)Cobalt(II) Tetrahydrate. *Aust. J. Chem.* **2000**, *53* (7), 601−605.

(15) Zheng, X.-F.; Shen, X.-Q.; Wan, X.-S.; Zhang, H.-Y.; Wang, H.; Yang, R.; Niu, C.-Y. Syntheses and Crystal Structures of Two Zn(II) Complexes, [Zn(Fura)2(2,2′-Bipy)(H_2O)] and [Zn(μ-Dnbc)$_2$] (Fura = Furoic Acid, 2,2′-Bpy = 2,2′-Bipyridine, Dnba = 3,5-Dinitrobenzoic Acid). *J. Coord. Chem.* **2007**, *60* (12), 1317−1325.

(16) Jin, S.; Huang, Y.; Wang, D.; Fang, H.; Wang, T.; Fu, P.; Ding, L. Non-Covalently Bonded 2D-3D Metal-Organic Frameworks from the Reactions of Cd(II) and Zn(II) with 3,5-Dimethylpyrazole and Carboxylate Ligands. *Polyhedron* **2013**, *60*, 10−22.

(17) Appavoo, D.; Omondi, B.; Guzei, I. A.; van Wyk, J. L.; Zinyemba, O.; Darkwa, J. Bis(3,5-Dimethylpyrazole) Copper(II) and Zinc(II) Complexes as Efficient Initiators for the Ring Opening Polymerization of ε-Caprolactone and d,l-Lactide. *Polyhedron* **2014**, *69*, 55−60.

(18) Lephoto, M. L.; Nakano, K.; Appavoo, D.; Owaga, B. O.; Nozaki, K.; Darkwa, J. Pyrazole Supported Zinc(II) Benzoates as Catalysts for the Ring Opening Copolymerization of Cyclohexene Oxide and Carbon Dioxide. *Catalysts* **2016**, *6* (1), 17.

(19) Nuñez-Dallos, N.; Posada, A. F.; Hurtado, J. Coumarin Salen-Based Zinc Complex for Solvent-Free Ring Opening Polymerization of ε-Caprolactone. *Tetrahedron Lett.* **2017**, *58* (10), 977−980.

(20) Labet, M.; Thielemans, W. Synthesis of Polycaprolactone: A Review. *Chem. Soc. Rev.* **2009**, *38* (12), 3484−3504.

(21) Torres, J. F.; Grattz, I.; Salcedo; Hurtado, J. Synthesis of polycaprolactone usable in biodegradable packaging production. *Agronomia Colombiana.* **2016**, *34* (1Supl), S185−S188.

(22) Posada, A. F.; Macías, M. A.; Movilla, S.; Miscione, G. P.; Pérez, L. D.; Hurtado, J. J. Polymers of ε-Caprolactone Using New Copper(II) and Zinc(II) Complexes as Initiators: Synthesis, Characterization and X-Ray Crystal Structures. *Polymers* **2018**, *10* (11), 1239.

(23) Castillo, K. F.; Bello-Vieda, N. J.; Nuñez-Dallos, N. G.; Pastrana, H. F.; Celis, A. M.; Restrepo, S.; Hurtado, J. J.; Ávila, A. G.; Castillo, K. F.; Bello-Vieda, N. J.; et al. Metal Complex Derivatives of Azole: A Study on Their Synthesis, Characterization, and Antibacterial and Antifungal Activities. *J. Braz. Chem. Soc.* **2016**, *27* (12), 2334−2347.

DOI: 10.1021/acs.cgd.9b00246
Cryst. Growth Des. 2019, 19, 3348−3357

(24) Sheldrick, G. M. Crystal Structure Refinement with SHELXL. *Acta Crystallogr., Sect. C: Struct. Chem.* **2015**, *71* (1), 3−8.
(25) Petříček, V.; Dušek, M.; Palatinus, L. Crystallographic Computing System JANA2006: General Features. *Z. Kristallogr. - Cryst. Mater.* **2014**, *229* (5), 345−352.
(26) Frisch, M. J.; Trucks, G. W.; Schlegel, H. B.; Scuseria, G. E.; Robb, M. A.; Cheeseman, J. R.; Scalmani, G.; Barone, V.; Mennucci, B.; Petersson, G. A.; et al. *Gaussian 09*, revision B.01.; Gaussian, Inc.: Wallingford, CT, 2009.
(27) Zhao, Y.; Truhlar, D. G. Hybrid Meta Density Functional Theory Methods for Thermochemistry, Thermochemical Kinetics, and Noncovalent Interactions: The MPW1B95 and MPWB1K Models and Comparative Assessments for Hydrogen Bonding and van Der Waals Interactions. *J. Phys. Chem. A* **2004**, *108* (33), 6908−6918.
(28) Zhao, Y.; Truhlar, D. G. Design of Density Functionals That Are Broadly Accurate for Thermochemistry, Thermochemical Kinetics, and Nonbonded Interactions. *J. Phys. Chem. A* **2005**, *109* (25), 5656−5667.
(29) Zhao, Y.; Tishchenko, O.; Truhlar, D. G. How Well Can Density Functional Methods Describe Hydrogen Bonds to π Acceptors? *J. Phys. Chem. B* **2005**, *109* (41), 19046−19051.
(30) Zhao, Y.; Truhlar, D. G. Density Functionals with Broad Applicability in Chemistry. *Acc. Chem. Res.* **2008**, *41* (2), 157−167.
(31) Bottoni, A.; Calvaresi, M.; Ciogli, A.; Cosimelli, B.; Mazzeo, G.; Pisani, L.; Severi, E.; Spinelli, D.; Superchi, S. Selective and Practical Oxidation of Sulfides to Diastereopure Sulfoxides: A Combined Experimental and Computational Investigation. *Adv. Synth. Catal.* **2013**, *355* (1), 191−202.
(32) Giacinto, P.; Bottoni, A.; Calvaresi, M.; Zerbetto, F. Cl(−) Exchange SN2 Reaction inside Carbon Nanotubes: C-H$\cdots\pi$ and Cl$\cdots\pi$ Interactions Govern the Course of the Reaction. *J. Phys. Chem. C* **2014**, *118* (9), 5032−5040.
(33) Giacinto, P.; Cera, G.; Bottoni, A.; Bandini, M.; Miscione, G. P. DFT Mechanistic Investigation of the Gold(I)-Catalyzed Synthesis of Azepino[1,2-a]Indoles. *ChemCatChem* **2015**, *7* (16), 2480−2484.
(34) Andrae, D.; Häußermann, U.; Dolg, M.; Stoll, H.; Preuß, H. Energy-Adjustedab Initio Pseudopotentials for the Second and Third Row Transition Elements. *Theoret. Chim. Acta.* **1990**, *77* (2), 123−141.
(35) Orza, J. M.; García, M. V.; Alkorta, I.; Elguero, J. Vibrational Spectra of 3,5-Dimethylpyrazole and Deuterated Derivatives. *Spectrochim. Acta, Part A* **2000**, *56* (8), 1469−1498.
(36) Amalanathan, M.; Rastogi, V. K.; Hubert Joe, I.; Palafox, M. A.; Tomar, R. Density Functional Theory Calculations and Vibrational Spectral Analysis of 3,5-(Dinitrobenzoic Acid). *Spectrochim. Acta, Part A* **2011**, *78* (5), 1437−1444.
(37) Aguilar-Parrilla, F.; Cativiela, C.; Villegas, M. D. D. de; Elguero, J.; Foces-Foces, C.; Laureiro, J. I. G.; Cano, F. H.; Limbach, H.-H.; Smith, J. A. S.; Toiron, C. The Tautomerism of 3(5)-Phenylpyrazoles: An Experimental (1H, 13C, 15N NMR and X-Ray Crystallography) Study. *J. Chem. Soc., Perkin Trans. 2* **1992**, No. 10, 1737−1742.
(38) Deka, K.; Laskar, M.; Baruah, J. B. Carbon-Nitrogen Bond Cleavage by Copper(II) Complexes. *Polyhedron* **2006**, *25* (13), 2525−2529.
(39) Jin, S.-W.; Ye, X.-H.; Jin, L.; Zheng, L.; Li, J.-W.; Jin, B.-P.; Wang, D.-Q. Syntheses and Structural Characterization of Nine Coordination Compounds Assembled from Copper Acetate, 3,5-Dimethylpyrazole and Carboxylates. *Polyhedron* **2014**, *81*, 382−395.
(40) Karmakar, A.; Bania, K.; Baruah, A. M.; Baruah, J. B. Role of Nitro-Substituent in Pseudo-Polymorphism and in Synthesis of Metal Carboxylato Complexes of Copper, Zinc and Manganese. *Inorg. Chem. Commun.* **2007**, *10* (8), 959−964.
(41) Groom, C. R.; Bruno, I. J.; Lightfoot, M. P.; Ward, S. C. The Cambridge Structural Database. *Acta Crystallogr., Sect. B: Struct. Sci., Cryst. Eng. Mater.* **2016**, *72* (2), 171−179.
(42) Báuza, A.; Frontera, A.; Mooibroek, T. J. π-Hole Interactions Involving Nitro Compounds: Directionality of Nitrate Esters. *Cryst. Growth Des.* **2016**, *16* (9), 5520−5524.
(43) Gagnon, E.; Maris, T.; Maly, K. E.; Wuest, J. D. The Potential of Intermolecular N···O Interactions of Nitro Groups in Crystal Engineering, as Revealed by Structures of Hexakis(4-Nitrophenyl)-Benzene. *Tetrahedron* **2007**, *63* (28), 6603−6613.
(44) Spackman, M. A.; McKinnon, J. J.; Jayatilaka, D. Electrostatic Potentials Mapped on Hirshfeld Surfaces Provide Direct Insight into Intermolecular Interactions in Crystals. *CrystEngComm* **2008**, *10* (4), 377−388.
(45) Jayatilaka, D.; Grimwood, D. J.; Lee, A.; Lemay, A.; Russel, A. J.; Taylor, C.; Wolff, S. K.; Cassam-Chenai, P.; Whitton, A. *TONTO*, a system for computational chemistry; University of Western Australia, 2005.
(46) Spackman, M. A.; Jayatilaka, D. Hirshfeld Surface Analysis. *CrystEngComm* **2009**, *11* (1), 19−32.
(47) Robinson, K.; Gibbs, G. V.; Ribbe, P. H. Quadratic Elongation: A Quantitative Measure of Distortion in Coordination Polyhedra. *Science* **1971**, *172* (3983), 567−570.
(48) Ozarowski, A.; Calzado, C. J.; Sharma, R. P.; Kumar, S.; Jezierska, J.; Angeli, C.; Spizzo, F.; Ferretti, V. Metal-Metal Interactions in Trinuclear Copper(II) Complexes [Cu3(RCOO)4-(H2TEA)2] and Binuclear [Cu2(RCOO)2(H2TEA)2]. Syntheses and Combined Structural, Magnetic, High-Field Electron Paramagnetic Resonance, and Theoretical Studies. *Inorg. Chem.* **2015**, *54* (24), 11916−11934.
(49) Valigura, D.; Melník, M.; Koman, M.; Martiška, L.; Korabik, M.; Mrozińsky, J.; Glowiak, T. Structural Confirmation of the 3,5-Dinitrosalicylato Anion Coordination Ability to Metal Ion: Crystal Structure, Spectral and Magnetic Properties of the $[Cu_3\{3,5\text{-}(NO_2)2sal_2\text{-}\}2\{3,5\text{-}(NO_2)2sal1\text{-}\}2(H_2O)_4]$. $4H_2O$. *Polyhedron* **2004**, *23* (15), 2447−2456.
(50) Xing, Y.-H.; Zhou, G.-H.; An, Y.; Zeng, X.-Q.; Ge, M.-F. Synthesis and Structure of a New Trinuclear Copper(II) Complex with 5-Phenyl Pyrazole-3-Carboxylic Acid as Ligand. *Synth. React. Inorg., Met.-Org., Nano-Met. Chem.* **2008**, *38* (6), 514−517.
(51) Gautier-Luneau, I.; Phanon, D.; Duboc, C.; Luneau, D.; Pierre, J.-L. Electron Delocalisation in a Trinuclear Copper(II) Complex: High-Field EPR Characterization and Magnetic Properties of $Na_3[Cu_3(Mal)3(H_2O)].8H_2O$. *Dalton Trans.* **2005**, No. 23, 3795−3799.
(52) Hurtado, J.; Ibarra, L.; Yepes, D.; García-Huertas, P.; Macías, M. A.; Triana-Chavez, O.; Nagles, E.; Suescun, L.; Muñoz-Castro, A. Synthesis, Crystal Structure, Catalytic and Anti-Trypanosoma Cruzi Activity of a New Chromium(III) Complex Containing Bis(3,5-Dimethylpyrazol-1-Yl)Methane. *J. Mol. Struct.* **2017**, *1146*, 365−372.
(53) Sandoval-Rojas, A. P.; Ibarra, L.; Cortés, M. T.; Hurtado, M.; Macías, M.; Hurtado, J. J. Synthesis and Characterization of a New Copper(II) Polymer Containing a Thiocyanate Bridge and Its Application in Dopamine Detection. *Inorg. Chim. Acta* **2017**, *459*, 95−102.

DOI: 10.1021/acs.cgd.9b00246
Cryst. Growth Des. 2019, 19, 3348−3357